American Journal of Environmental Science and Engineering
2024, Vol. 8, No. 3, pp. 49-64
https://doi.org/10.11648/j.ajese.20240803.11

Research Article

Gully Erosion Risk Assessment Using a GIS-Based Bivariate Statistical Models and Machine Learning in the Dodota Alem Watershed, Ethiopia

Gizaw Tesfaye*, Daniel Bekele, Melat Eshetu, Mohamed Rabo, Abebe Bezu, Abera Asefa

Ethiopian Institute of Agricultural Research (EIAR), Melkassa Agricultural Research Center, Adama, Ethiopia

Abstract

One of the most significant environmental hazards threatening ecosystems is gully erosion. In this study, we applied two bivariate statistical models—frequency ratio (FR) and index of entropy (IoE)—as well as a machine learning algorithm (RF) to generate gully erosion susceptibility maps (GESM). The study was conducted in the Dodota Alem watershed of the Awash River basin, covering 135 km². Our modeling utilized input data from field surveys, Google Earth, and secondary sources. Geo-environmental factors such as land use and land cover, soil characteristics, altitude, slope, aspect, profile curvature, plan curvature, drainage density, distance from roads, distance from streams, stream power index (SPI), and topographic wetness index (TWI) were considered after a multi-collinearity test. Among these factors, distance from roads had the most substantial impact on gully erosion susceptibility according to the RF model, while SPI played a crucial role in the FR and IoE models. Approximately 60% of the watershed falls into the moderate or high susceptibility category for gully erosion using the FR and IoE models, whereas the RF model projected the largest area in the very high susceptibility class. Validation results, based on the Area Under Curve (AUC), demonstrated prediction efficiencies of 0.912 (FR), 0.880 (IoE), and 0.932 (RF). These findings can guide decision-makers and planners in implementing effective soil and water conservation measures to mitigate the damage caused by gully erosion. Additionally, this approach serves as a valuable reference for future research on gully erosion susceptibility.

Keywords

Gully Erosion, Machine Learning, Random Forest, Bivariate Models, Ethiopia

1. Introduction

Runoff-induced soil erosion is a major contributor to global land degradation. For instance, it affects agricultural lands, leads to soil fertility decline, and results in sediment deposition in reservoirs [36]. Despite occupying a small percentage of a watershed, gully erosion generates significant environmental and socioeconomic problems by impairing soil and land functionality [28, 54]. Gully erosion also exacerbates floods, lowers water tables, contributes to desertification, and transports large amounts of sediment from watersheds to coastal and lowland areas, causing severe damage to infra-

*Corresponding author: gzwtesfaye@gmail.com (Gizaw Tesfaye)

Received: 12 August 2024; **Accepted:** 4 September 2024; **Published:** 23 September 2024

structure [5, 9, 35]. Due to its ability to rapidly erode and transfer substantial soil volumes, gully erosion is highly destructive [2].

Ethiopia faces rapid soil erosion rates [51]. Previous research indicates that annual soil erosion varies from 16 to 220 tons per hectare, depending on land use and agro-ecology [27, 51]. Factors contributing to this erosion include high population pressure, intense tropical rains with erosive potential, rugged topography, extensive deforestation for fuelwood, cultivation expansion into steep and erosion-prone areas, and inadequate integrated catchment management [61]. In the northern Ethiopian highlands, gully erosion accounts for up to 28% of soil loss [43]. Addressing substantial gully erosion is crucial for ongoing and future environmental and water management projects in Ethiopia, ranging from small-scale irrigation to large hydropower dams [22, 25, 52].

To mitigate these challenges, it is essential to identify gully erosion-prone areas accurately. Several gully erosion models aid in susceptibility mapping (GESM), utilizing relationships between gully occurrence and geo-environmental factors [49]. Data-driven knowledge-based, statistical, and machine learning models have successfully predicted GESM worldwide [2, 14, 21, 23, 29, 49]. Machine learning algorithms offer excellent accuracy for susceptibility assessment [2].

While some studies have explored gully erosion susceptibility mapping in Ethiopia [1, 11], none have focused on the Awash River Basin—a critical, intensively utilized, and environmentally vulnerable region [7]. This study employs bivariate statistical models and machine learning algorithms to analyze geo-environmental characteristics, producing a gully susceptibility map. By evaluating three models and comparing results, we aim to enhance mapping efficiency in a region heavily impacted by gully erosion. Ultimately, our research informs strategies for preventing gully erosion and environmental degradation.

2. Materials and Methods

2.1. Description of the Study Area

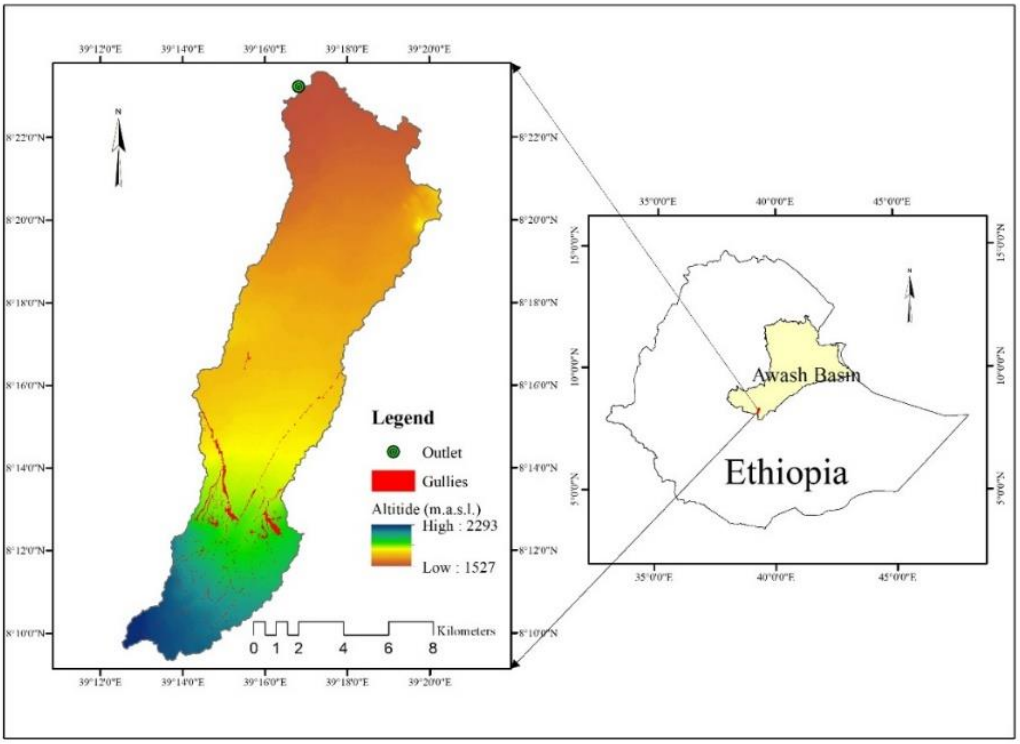

Figure 1. *Location and gullies map of Dodota Alem watershed in the Awash Basin.*

The study was conducted at the Dodota Alem watershed (geographically located 8 °09' to 8 °23' N and 38 °12' to 38 °20' E) situated in the central rift valley of Ethiopia, 125 km southeast of Addis Ababa. The catchment area of the Dodota Alem watershed is 135 km^2 and is found in the Awash River basin. The elevation of the watershed varies from 1527 to 2293 meters above sea level (Figure 1). The slope gradient varies from flatlands on the valley bottom to very steep slopes in the surrounding mountain ranges. The location has a bimodal rainfall distribution with a mean annual rainfall of 804

mm. The annual mean minimum and maximum temperatures are 13 ℃ and 28 ℃, respectively [55]. According to [20], the dominant soils in the upper part of the watershed are vertic cambisols and mollic andosols. The lower part is dominated by eutric fluvisols and eutric regosols, the middle is dominated by eutric regosols. The watershed consists of cultivable land (88.9%), settlement (0.3%), shrub land (0.1%), and degraded land (10.7%) (Figure 2a).

2.2. Methods

Gully inventory datasets

In this study, a gully erosion inventory map of the study region was generated using field surveys, Google Earth, and available reports obtained from secondary data (Figure 1). The geographical location of gullies was recorded using GPS. A total of 108 gullies were identified and mapped using the ArcGIS environment. About 76 (70%) gullies were chosen for training of the model, and 32 (30%) were used for validation [15].

Gully erosion factors

Gully erosion occurrence and behavior depend on several factors, including environmental, geological, geomorphological, and hydrological factors. Selecting gully erosion factors is an important component in preparing the gully erosion susceptible maps (GESMs) using various methods [48]. In this study, twelve gully erosion factors, namely land use and land cover (LULC), soil, altitude, slope, aspect profile curvature, plan curvature, drainage density, distance from road, distance from stream, stream power index (SPI), and topographic wetness index (TWI) were used for gully erosion modeling. The selection of parameters was made based on geomorphological knowledge of gully erosion phenomena in the study area and multi-collinearity analysis. Due to the small size of the study area, climatic conditions have been considered homogeneous and, therefore, no climatic attributes were used to build the model.

Land use and land cover (LULC) is one of the important factors that set the threshold for gully initiation [6]. In this study, generally, the LULC map of the watershed was generated based on Landsat 8 satellite data (30 m spatial resolution) sensed on February 24, 2022. Pixel-based supervised image classification using the maximum likelihood algorithm was used to create the map. Four land cover types were extracted, such as cultivated land, degraded land, settlements and shrub land (Figure 2a). The produced LULC was validated using 275 randomly selected samples from ground truth collected from the field and Google Earth. The accuracy (Kappa coefficient) of the generated map is 83.5% [18]. Thus, in this study, soil type was used as a controlling factor (Figure 2b). The soil type was extracted from the FAO soil map [20].

Topographic factors are very important geomorphological factors that affect gully erosion [5, 23]. The ten topographic attributes (slope, stream power index, topographic wetness index, plan curvature, profile curvature, drainage density, distance from road, distance from stream, altitude, and aspect) were extracted from the Advanced Land Observing Satellite (ALOS PALSAR) Digital Elevation Model (DEM) with 12.5m resolution (https://search.asf.alaska.edu/) using ArcGIS.

The altitude of the area determines vegetation distribution and rainfall patterns, which indirectly affect gully distribution [31, 60]. The study area's altitude varies from 1527 to 2293 meters above sea level (Figure 2c). Slope directly affects gully erosion by influencing the velocity of runoff and the opportunities for infiltration [48], which was subsequently classified into four classes (Figure 2d). An aspect map of the watershed is classified as flat, north, south, east, west, northeast, southeast, southwest, and northwest (Figure 2e). Aspect controls the duration of sunlight, moisture, evaporation, and transpiration, and the distribution of vegetation that indirectly affects the gully erosion process [29, 56].

The change in slope inclination or aspect is plan curvature [46]. Plan curvature can have positive, negative, or zero values to represent convexity, concavity, or flatness, respectively [14] (Figure 2f). The surface curvature in the direction of the steepest slope is called the profile curvature. It changes the velocity of water flow that drains the surface and affects erosion and sediment deposition [48]. Positive and negative values indicate the concavity and convexity of slope curvature, respectively, and zero values are flat surfaces. The value ranges in the study area between – 5.8 and 3.8 (Figure 2g).

Drainage density is a measure of stream length per unit of area and depends on lithology, permeability, vegetation cover, and soil type [37]. The values of drainage density in the study area vary from 0 to 5 (km/km^2) (Figure 2h). Distance from the road is an important factor for the occurrence of gully erosion [15, 47]. Roads will aggravate the gully erosion process through their interruption and concentrate of overland flow [15]. Roads were extracted from 1:50,000-scale topographical maps [18]. It was divided into four different zones (Figure 2i). Gullies are associated with a stream network [15]. Using the natural break classification technique, four buffer zones are created to determine the effect of streams on gullies (Figure 2j).

The Stream Power Index (SPI) measures the erosion power of the stream. Areas with high stream power have high erosion potential [23] (Figure 2k). The SPI can be defined using equation 1, [40].

$$SPI = A_{s\times}\ tan\,\beta \quad (1)$$

Where, A_S is the specific catchment's area and β is the local slope gradient measured in degrees.

Topographic Wetness Index (TWI) indicates the effect of topography on the location and size of saturated source areas of runoff generation [23] (Figure 2l). It is based on the assumption of steady state conditions and uniform soil properties. TWI is defined using equation 2 [8].

$$TWI=\ln\frac{S}{\tan\alpha} \quad (2)$$

Where, S is the cumulative upslope area draining through point (per unit contour length) and α is the slope gradient (in degrees).

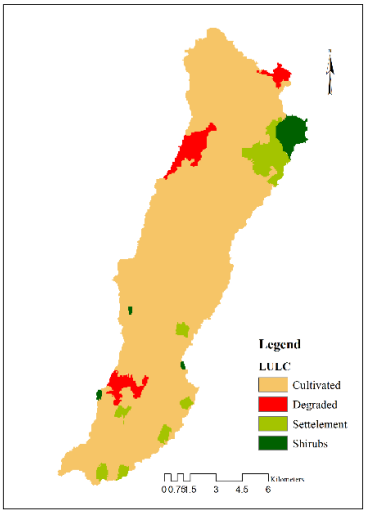

a

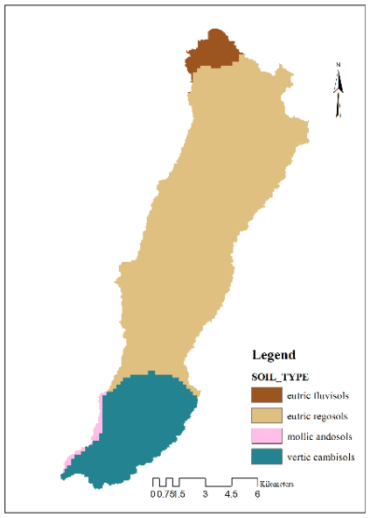

b

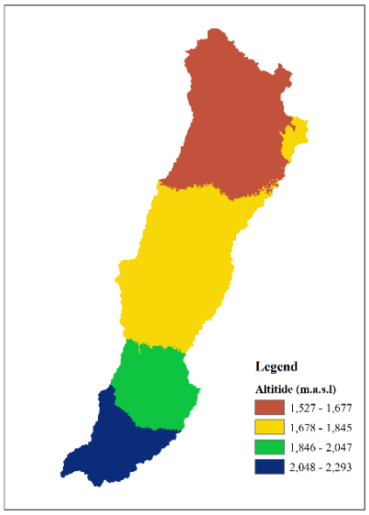

c

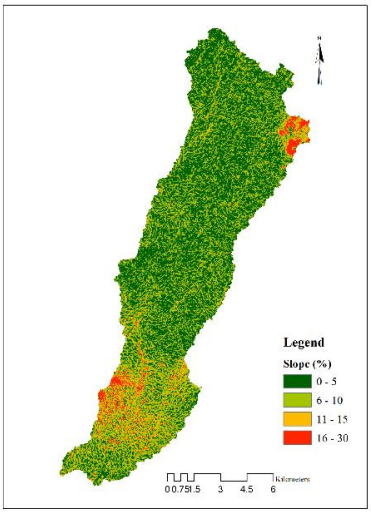

d

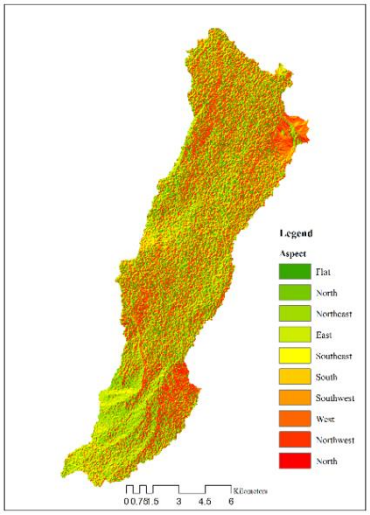

e

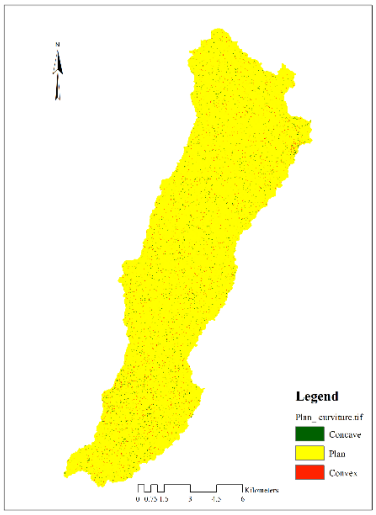

f

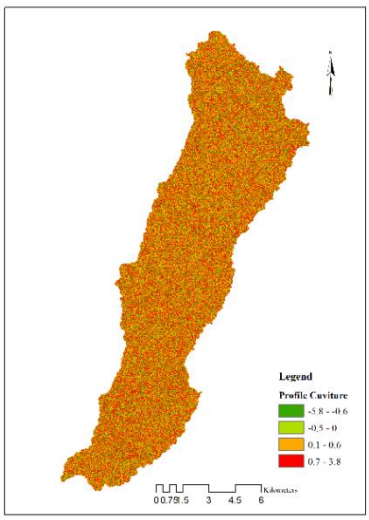

g

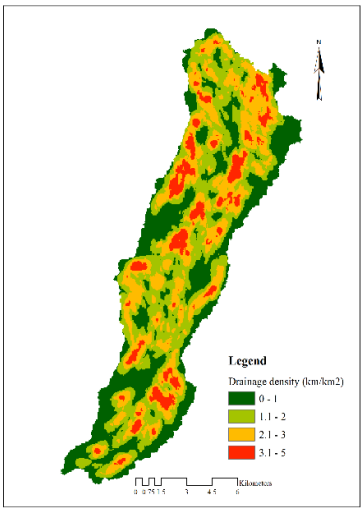

h

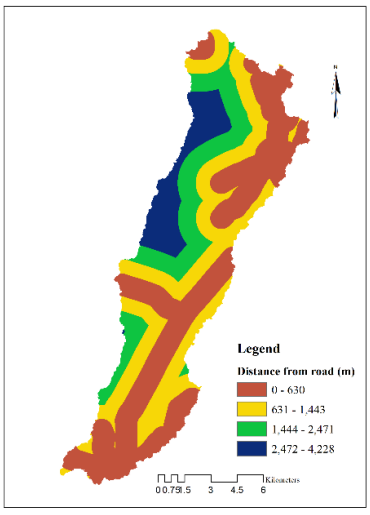

i

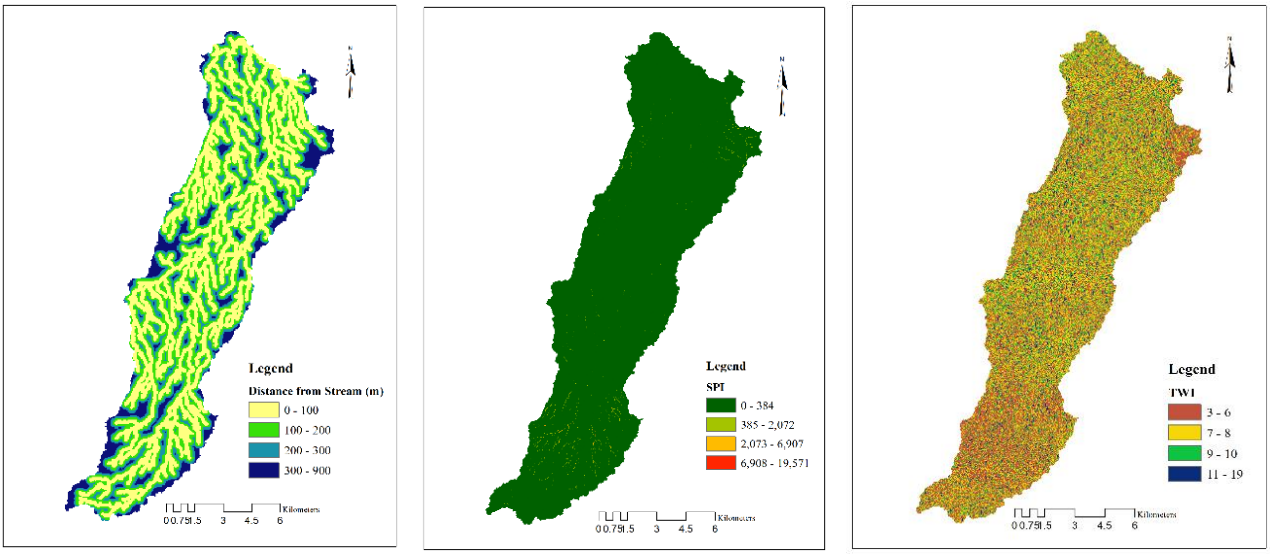

j k l

Figure 2. *Spatial thematic maps of gully conditioning factors at Dodota Alem watershed: a) land use and land cover (LULC), b) soil type, c) altitude, d) slope, e) aspect f) profile curvature, g) plan curvature, h) drainage density, i) distance from road, j) distance from stream, k) stream power index (SPI) and l) topographic wetness index (TWI).*

Multi-collinearity analysis

In this study, multi-collinearity was tested by combining results from the variance inflation factor (VIF) and tolerance (TOL), which are commonly used in different fields, including gully erosion [5, 50]. Since, multi-collinearity was evaluated using VIF, which represents the multiplicative inverse of TOL, calculated as $1 - r^2$, where r^2 is obtained by the regression of each variable for the remaining variables. When values of TOL and VIF are ≤ 0.1 and ≥ 5 this indicates multi-collinearity among independent variables, respectively [18].

Models for gully erosion susceptibility mapping

The frequency ratio (FR), Index of entropy (IoE), and random forest (RF) models were used to build the GESM. It was finally classified as "low", "moderate", "high", and "very high" using the natural break method using ArcGIS [30]. This classification method was selected as it reduces variance within a class. The RF model was also utilized to rank the most valuable gully erosion predictor factor.

Frequency ratio model (FR)

The Frequency ratio is a bivariate statistical method and a simple geospatial assessment tool for identifying the probabilistic relationship between dependent and independent factors [49]. FR is the ratio of gully erosion probability of occurrence to non-occurrence within a gully predictor factor class. The FR can be described as in equation 3 [5]:

$$FR = (A/B)/(C/D) \quad (3)$$

Where, A is the number of gully erosion pixels for each class of predictor factors, B is the total number of gully erosion pixels in the study area, C is the number of pixels in each class of gully predictor factor, and D is the number of total pixels in the study area.

Index of entropy (IoE)

The second bivariate approach which was used for assessing gully susceptibility is an index of entropy model. The theory of entropy expresses the extent of the disorder, instability, uncertainty, and imbalance of a system [17, 58]. In this method, the value of each factor is considered as "Entropy Index". As a result, the entropy value can be used to calculate the objective weights of the index system following Equations 4-9 have been used [17]:

$$P_{ij} = \frac{b}{a} \quad (4)$$

$$(P_{ij}) = \frac{P_{ij}}{\sum_{j=1}^{Sj} P_{ij}} \quad (5)$$

$$H_j = -\sum_{i=1}^{Sj}(P_{ij}) \log_2(P_{ij}), J = 1, \ldots, n \quad (6)$$

$$H_{j\,max} = \log_2 S_j \quad (7)$$

$$I_j = \frac{H_{j\,max} - H_j}{H_{J\,max}}, I = (0,1), J = 1, \ldots, n \quad (8)$$

$$W_j = I_j + P_{ij} \quad (9)$$

where a and b are the domain and gully erosion percentages, respectively, (P_{ij}) is the probability density, H_j and $H_{j\ max}$ indicate the entropy values and maximum entropy, respectively, I_j is the information value, S_j is the number of classes and W_j indicates the resulting weight of factor. W_j's values range from 0 to 1. One advantage of index of entropy model is that it determines weights for each factor based on its in-

fluence on the model performance after its removal; the more it affects the performance, it would gain a higher weight.

Random Forest (RF)

Random Forest (RF) is a multivariate nonparametric machine learning technique developed by [10]. The model is often used to solve multiple problems related to classification and prediction [53]. The RF algorithm uses binary trees, which use a set of observations via bootstrapping techniques. Every tree was trained using two thirds of the randomly selected training samples, while the remaining one third of the training samples, called out-of-bag (OOB) samples, were used to test the model result [1]. The RF is a powerful decision tree classifier that predicts well when there is missing data, avoids over-fitting problems, produces more stable results, and is less sensitive to multi-collinearity than other machine learning algorithms [13, 19, 32, 38]. It is also known for predicting gully erosion very well compared to other machine learning algorithms [21].

The RF utilizes two types of errors, mean decrease accuracy (MDA) and mean decrease Gini (MDG) index in the ranking of factors. The MDA plot illustrates how much accuracy the model loses by excluding each variable. The more the accuracy suffers, the more important the variable is for the successful classification. The MDG is a measure of how each factor contributes to the uniformity of the nodes and leaves in the resulting random forest. The higher the value of the MDA or MDG score, the greater the importance of the variable in the model [38]. In this study, the 'random forest' package in R 4.2.0 [34] was utilized to implement the RF algorithm.

2.3. Accuracy Assessment

In this study, model performance was assessed using the area under the ROC curve (AUC). The ROC (receiver operating characteristic) curve and the AUC (area under the curve) were used to validate and the assess accuracy of the models [15]. ROC is used for evaluating the predictive accuracy of a chosen model. The AUC identifies the model performance by predicting the occurrence or nonoccurrence of gullies. The most accurate model has a curve with the highest AUC [15]. This method has been successfully used in gully erosion prediction research [2, 26, 49].

3. Results and Discussion

3.1. Multi-Collinearity Test

The result of the multi-collinearity test showed that VIF ranges from 1.26 to 2.96, while the TOL varies from 0.34 to 0.80 (Table 1). VIF values greater than 5 or 10, with corresponding TOL values less than 0.1, indicate serious multi-collinearity among factors [44]. This analysis showed that the TOL and VIF of the 12 factors were greater than 0.1 and less than 5, respectively. which indicates there is no multi-collinearity among these factors.

Table 1. *Multi-collinearity test statistics of gully predictor variables.*

Conditional factor	Multi-collinearity	
	Tolerance	VIF
Altitude	0.527	1.897
Aspect	0.360	2.779
Profile curvature	0.353	2.834
Plan curvature	0.638	1.568
Drainage density	0.337	2.963
Distance from road	0.458	2.185
Distance from stream	0.375	2.669
LULC	0.605	1.652
Slope	0.380	2.633
Soil	0.565	1.770
SPI	0.796	1.257
TWI	0.356	2.808

Results of frequency ratio model (FR)

The FR values were estimated based on the spatial relationship of gully erosion locations and the twelve conditioning factors. As shown in Table 2, when a class of a factor has the FR value higher than 1, it is assumed that the class is susceptible to gully erosion [5]. A frequency ratio model revealed that most gully erosion occurs at elevations of 1846 to 2047 m (5.05). The elevation range of 2048 to 2293 m has a FR value of 1.06. Elevations between 1527 and 1677 m had the lowest frequency ratio (0.00). Based on FR values, the southwest and south aspects had the highest susceptibility to gully erosion, with a value of 2.89 and 1.95, respectively. The lowest values were found in the flat (0.35) and southeast (0.54) part of the watershed. which is primarily due to denser vegetation cover compared to southwest and south aspect [57, 60]. The correlation between profile and plan curvatures and gully erosion showed that the concave plan and convex slopes had the highest FR values, 1.87 and 1.03, respectively. However, less influence is found when the curvature is zero or plain. Runoff accumulation and subsequent flow could exacerbate gully erosion [1, 21].

There is an increasing trend in FR values with increasing drainage density factor values. The highest FR value for the drainage density factor classes is 2.04 (3.1–5.0 km/km^2) and the smallest FR value is 0.85 (0-1 km/km^2). In general, this can be explained by the relationship between high drainage density and increased runoff, which eventually increases the likelihood of gully erosion [49]. The highest FR value for the

distance of the road factor is 1.61 for the class of 631 to 1443 m, followed by the next class (1.16). In the case of distance from the stream, the highest FR value is 1.52 for class of 0 to 100 m, followed by the second class (0.55). The lower FR values is explained by other studies that indicated the association between the development of gullies and their proximity to rivers and roads has an inverse trend [15].

Among the different LULC, the degraded and cultivated land categories had the highest FR values (2.45 and 1.01), indicating maximum gully susceptibility. This demonstrates how vegetation has a detrimental impact on gully formation since it can limit surface runoff and, consequently, gully erosion. This result is consistent with [62], which found that compared to bare and agricultural regions, forested areas experience less erosion in the form of gullies. In the case of slope, the 16 to 30% classes have a FR value of 3.38, while the classes with slopes of between 0 to 5 % have the lowest FR values, 0.52. In some regions, gullies are also common features in hilly areas with steep slopes because of high run-off velocities [24, 54, 59].

The relationship between soil type and gully occurrence showed that areas with Vertic cambisols have high sensitivity to gully erosion, with the highest FR value of 2.88, followed by Mollic andosols with the FR value of 0.80. According to [42], Vertisols are more susceptible to gully erosion because of their high propensity for swelling and shrinkage. The fourth class of the SPI had the highest FR value (2.11), while the first class (0 to 384) had the lowest FR value (0.99). According to [41], SPI represents the catchment area of concentrated runoff; hence, the higher the SPI, the greater the chance of a gully occurring. In the present scenario, the first class of TWI had a greater FR value (FR = 1.29), followed by the fourth (FR = 0.94). According to [45], non-uniform topography within small catchments is a major factor controlling the spatial variability of soil water, and the location and development of gullies.

Table 2. *Spatial relationship between class of each conditioning factor and gully erosion using FR.*

Factor	Class	Total Pixels		Gully Pixel		FR
		Number	%	Number	%	
Altitude	1527 - 1677	304,286	35.2	-	0.0	0.000
	1678 - 1845	334,109	38.7	1,998	16.7	0.432
	1846 - 2047	120,226	13.9	8,416	70.3	5.054
	2048 - 2293	105,529	12.2	1,554	13.0	1.063
Aspect	Flat (-1)	62,051	7.8	331	2.8	0.354
	North (0 °to 22.5 °)	112,050	14.1	1,523	12.7	0.902
	Northeast (22.5 °to 67.5 °)	164,951	20.8	2,660	22.2	1.071
	East (67.5 °to 112.5 °)	96,244	12.1	1,574	13.2	1.086
	Southeast (112.5 °to 157.5 °)	59,193	7.5	482	4.0	0.541
	South (157.5 °to 202.5 °)	7,604	1.0	223	1.9	1.947
	Southwest (202.5 °to 247.5 °)	10,149	1.3	442	3.7	2.891
	West (247.5 °to 292.5 °)	81,763	10.3	1,147	9.6	0.931
	Northwest (292.5 °to 337.5 °)	158,914	20.0	2,700	22.6	1.128
	North (337.5 °to 360 °)	41,325	5.2	881	7.4	1.415
Profile curvature	-5.8 - -0.6	139,907	16.2	1,974	16.7	1.034
	-0.5 - 0	162,262	18.8	2,206	18.7	0.997
	0.1 - 0.6	256,892	29.7	3,438	29.2	0.981
	0.7 - 3.8	305,089	35.3	4,169	35.4	1.002
Plan curvature	Concave	10,042	1.2	260	2.2	1.870
	Plan	844,334	97.7	11,538	96.4	0.987
	Convex	9,774	1.1	165	1.4	1.219

Factor	Class	Total Pixels		Gully Pixel		FR
		Number	%	Number	%	
Drainage density	0-1	263,820	30.5	3,094	25.9	0.847
	1.1-2	289,211	33.5	3,469	29.0	0.866
	2.1-3	239,404	27.7	3,381	28.3	1.020
	3.1-5	71,629	8.3	2,020	16.9	2.037
Distance from Road	0 - 630	361,326	41.8	3,643	30.9	0.739
	631 - 1443	259,563	30.0	5,714	48.5	1.614
	1444 - 2471	149,655	17.3	2,362	20.0	1.157
	2472 - 4228	93,606	10.8	68	0.6	0.053
Distance from stream	0 - 100	398,074	46.0	8,363	69.8	1.517
	100 - 200	258,492	29.9	1,965	16.4	0.549
	200 - 300	125,907	14.6	945	7.9	0.542
	300 - 900	82,059	9.5	701	5.9	0.617
LULC	Settlement	46,360	5.4	38	0.3	0.060
	Shrubs	19,956	2.3	9	0.1	0.033
	Degraded	37,910	4.4	1,266	10.7	2.445
	Cultivable	757,951	87.9	10,465	88.9	1.011
Slope	0 - 5%	446,883	51.8	3,109	26.8	0.517
	6 - 10%	325,212	37.7	5,179	44.6	1.183
	11 - 15%	65,468	7.6	2,192	18.9	2.488
	16 - 30%	24,615	2.9	1,122	9.7	3.387
Soil	Eutric fluvisols	30,857	3.6	-	0.0	0.000
	Eutric regosols	649,208	75.2	4,733	40.6	0.541
	Mollic andosols	7,796	0.9	84	0.7	0.799
	Vertic cambisols	175,985	20.4	6,833	58.7	2.879
SPI	0 - 384	859,444	99.5	11,440	98.3	0.988
	385 - 2072	4,312	0.5	164	1.4	2.823
	2073 - 6907	365	0.0	36	0.3	7.321
	6908 - 19571	29	0.0	2	0.0	5.119
TWI	3 - 6	301,814	34.9	5,263	45.2	1.294
	7 - 8	369,035	42.7	4,264	36.6	0.858
	9 - 10	131,715	15.2	1,336	11.5	0.753
	11 - 19	61,586	7.1	779	6.7	0.939

Results of index of entropy (IoE)

Table 3 shows the relationship between parameters and gully erosion locations by the index of entropy model. Altitude, SPI, LULC, soil, and TWI variables, with corresponding weights of 0.84, 0.55, 0.42, and 0.42, have a major effect on gully erosion. With scores of 0.001, 0.07, and 0.07, respectively, profile curvature, drainage density, and distance from stream had the least effect on gully erosion. In Table 3,

the Pij values of all factors (land use and land cover (LULC), soil, altitude, slope, aspect profile curvature, plan curvature, drainage density, distance from road, distance from stream, stream power index (SPI), and topographic wetness index (TWI)) show comparable results with the FR model. Previous studies have also evaluated the effectiveness of applying an index of entropy model for gully erosion susceptibility mapping [4, 3, 60]. Finally, GESM was calculated by summing each weighted factor to generate a gully erosion susceptibility map.

Table 3. *Spatial relationship between each conditioning factor and gully erosion using IoE model.*

Factor	Class	Total Pixels		Gully Pixel		P_{ij}	(P_{ij})	H_j	Hj_{max}	I_j	W_j
		Number	%	Number	%						
Altitude	1527 – 1677	304,286	35.2	-	0.0	0.000	0.000	0.973	2.000	0.513	0.841
	1678 – 1845	334,109	38.7	1,998	16.7	0.432	0.066				
	1846 – 2047	120,226	13.9	8,416	70.3	5.054	0.772				
	2048 – 2293	105,529	12.2	1,554	13.0	1.063	0.162				
Aspect	Flat (-1)	62,051	7.8	331	2.8	0.354	0.029	3.111	3.322	0.063	0.078
	North (0 ٩to 22.5 ٩)	112,050	14.1	1,523	12.7	0.902	0.074				
	Northeast (22.5 °to 67.5 ٩)	164,951	20.8	2,660	22.2	1.071	0.087				
	East (67.5 °to 112.5 ٩)	96,244	12.1	1,574	13.2	1.086	0.089				
	Southeast (112.5 °to 157.5 ٩)	59,193	7.5	482	4.0	0.541	0.044				
	South (157.5 °to 202.5 ٩)	7,604	1.0	223	1.9	1.947	0.159				
	Southwest (202.5 °to 247.5 ٩)	10,149	1.3	442	3.7	2.891	0.236				
	West (247.5 °to 292.5 ٩)	81,763	10.3	1,147	9.6	0.931	0.076				
	Northwest (292.5 °to 337.5 ٩)	158,914	20.0	2,700	22.6	1.128	0.092				
	North (337.5 °to 360 ٩)	41,325	5.2	881	7.4	1.415	0.115				
Profile Curvature	-5.8 - -0.6	139,907	16.2	1,974	16.7	1.034	0.258	1.9997	2.000	0.0001	0.0001
	-0.5 – 0	162,262	18.8	2,206	18.7	0.997	0.248				
	0.1 - 0.6	256,892	29.7	3,438	29.2	0.981	0.244				
	0.7 - 3.8	305,089	35.3	4,169	35.4	1.002	0.250				
Plan curvature	Concave	10,042	1.2	260	2.2	1.870	0.286	1.379	1.585	0.130	0.176
	Plan	844,334	97.7	11,538	96.4	0.987	0.151				
	Convex	9,774	1.1	165	1.4	1.219	0.186				
Drainage Density	0-1	263,820	30.5	3,094	25.9	0.847	0.178	1.890	2.000	0.055	0.066
	1.1-2	289,211	33.5	3,469	29.0	0.866	0.182				
	2.1-3	239,404	27.7	3,381	28.3	1.020	0.214				
	3.1-5	71,629	8.3	2,020	16.9	2.037	0.427				
Distance from Road	0 – 630	361,326	41.8	3,643	30.9	0.739	0.207	1.606	2.000	0.197	0.176
	613 – 1443	259,563	30.0	5,714	48.5	1.614	0.453				
	1444 – 2471	149,655	17.3	2,362	20.0	1.157	0.325				
	2472 – 4228	93,606	10.8	68	0.6	0.053	0.015				
Distance from stream	0 – 100	398,074	46.0	8,363	69.8	1.517	0.470	1.835	2.000	0.082	0.066
	100 – 200	258,492	29.9	1,965	16.4	0.549	0.170				

Factor	Class	Total Pixels		Gully Pixel		P_{ij}	(P_{ij})	H_j	Hj_{max}	I_j	W_j
		Number	%	Number	%						
LULC	200 – 300	125,907	14.6	945	7.9	0.542	0.168				
	300 – 900	82,059	9.5	701	5.9	0.617	0.191				
	Settlement	46,360	5.4	38	0.3	0.060	0.017	1.049	2.000	0.476	0.422
	Shrubs	19,956	2.3	9	0.1	0.033	0.009				
	Degraded	37,910	4.4	1,266	10.7	2.445	0.689				
	Cultivated	757,951	87.9	10,465	88.9	1.011	0.285				
Slope	0 - 5%	446,883	51.8	3,109	26.8	0.517	0.068	1.730	2.000	0.135	0.256
	6 - 10%	325,212	37.7	5,179	44.6	1.183	0.156				
	11 - 15%	65,468	7.6	2,192	18.9	2.488	0.328				
	16 - 30%	24,615	2.9	1,122	9.7	3.387	0.447				
Soil	Eutric fluvisols	30,857	3.6	-	0.0	0.000	0.000	1.212	2.000	0.394	0.416
	Eutric regosols	649,208	75.2	4,733	40.6	0.541	0.128				
	Mollic andosols	7,796	0.9	84	0.7	0.799	0.189				
	Vertic cambisols	175,985	20.4	6,833	58.7	2.879	0.682				
SPI	0 – 384	859,444	99.5	11,440	98.3	0.988	0.061	1.728	2.000	0.136	0.554
	385 – 2072	4,312	0.5	164	1.4	2.823	0.174				
	2073 – 6907	365	0.0	36	0.3	7.321	0.450				
	6908 – 19571	29	0.0	2	0.0	5.119	0.315				
TWI	3 – 6	301,814	34.9	5,263	45.2	1.294	1.000	1.184	2.000	0.408	0.392
	7 – 8	369,035	42.7	4,264	36.6	0.858	0.663				
	9 – 10	131,715	15.2	1,336	11.5	0.753	0.582				
	11 – 19	61,586	7.1	779	6.7	0.939	0.725				

Results of random forest (RF)

To prioritize the conditioning factors of gully erosion susceptibility, MDA and MDG errors were calculated (Figure 3, Table 4). Results showed that drainage density (4.97), altitude (4.94) and distance from road (4.84) are the greatest impact on gully erosion whereas SPI (0.49) and plan curvature (-1.00) are least contributing factors based on MDA. According to MDG distance from road (0.42), LULC (0.39), and soil type (0.38) hold the greatest importance on gully erosion occurrence whereas plan curvature (0.05) and SPI (0.03 had the lowest important. MDA and MDG errors in random forest algorithm have been commonly utilize in many fields and showing a good performance for factor importance [12, 16, 19, 33, 49]. Consequently, using ArcGIS, gully erosion susceptibility map (GESM) was created and classified into four classes including low, moderate, high, and very high susceptibility according to natural break method.

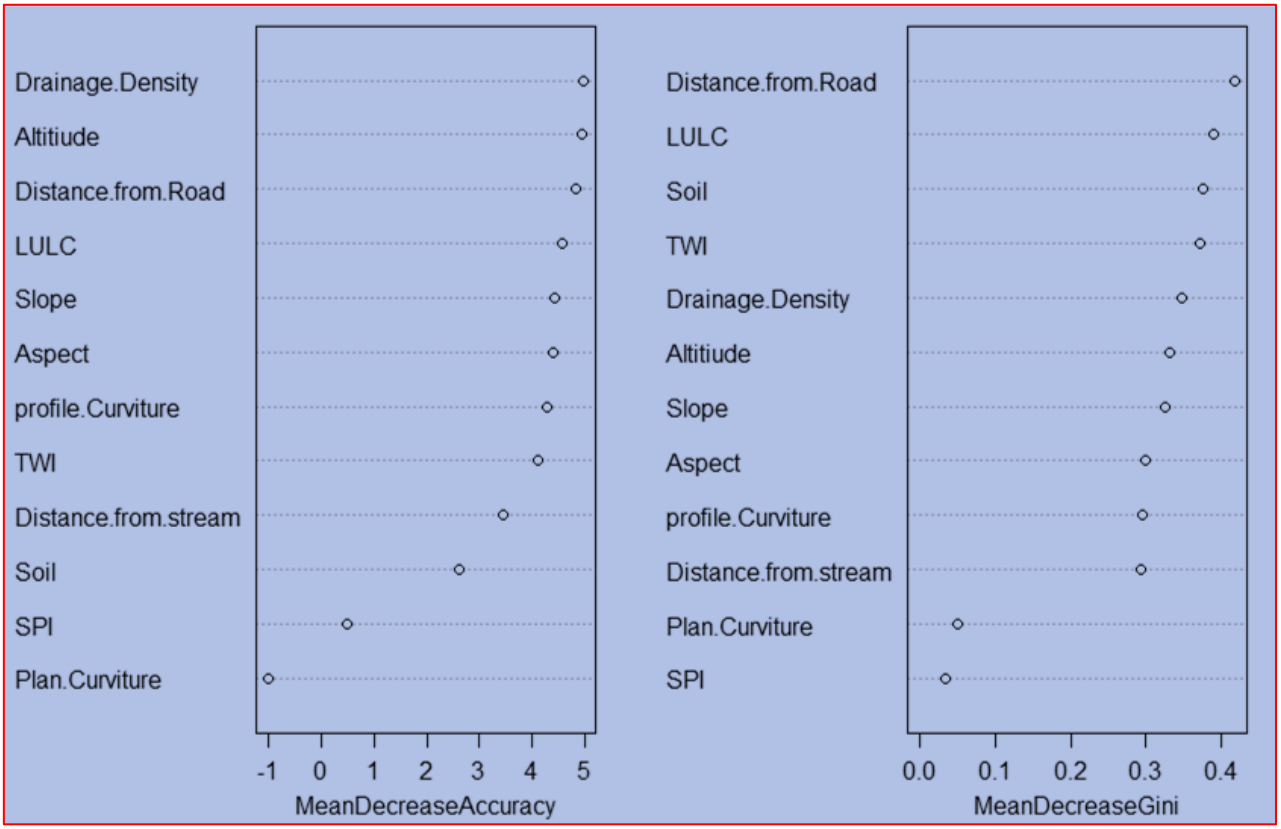

Figure 3. *Two measures of variable importance (MDA and MDG) calculated by the random forest algorithm.*

Table 4. *Conditioning factors of importance based on the random forest model.*

Factors	0	1	MDA	MDG
Altitude	4.70	4.71	4.94	0.33
Aspect	4.35	4.33	4.40	0.30
Profile curvature	4.28	4.21	4.29	0.30
Plan curvature	-1.00	-1.00	-1.00	0.05
Drainage density	4.87	4.79	4.97	0.35
Distance from road	4.76	4.66	4.84	0.42
Distance from stream	3.34	3.32	3.44	0.29
LULC	4.40	4.39	4.56	0.39
Slope	4.35	4.40	4.42	0.33
Soil	2.54	2.58	2.61	0.38
SPI	0.73	0.00	0.49	0.03
TWI	4.00	3.88	4.10	0.37

MDA= Mean decrease accuracy; MDG=Mean decrease Gini; 1= Gully presence and 0=Gully absence

3.2. Gully Erosion Susceptibility Maps (GESMs)

Through the use of bivariate statistical models (FR and index of entropy) and machine learning with random forest, the susceptibility to gully erosion was compared. According to the FR approach, gully erosion was classified with low, moderate, high, and very high classes of susceptibility with an area coverage of 34.9%, 32.4%, 25.1%, and 7.6% of the total area of the Dodota Alem watershed, respectively (Table 5) (Figure 4). Most of the watershed area falls into low (37.5%) and moderate (37.3%) gully erosion susceptibility classes according to the IoE model. High and very high susceptible classes accounted for only 20.9% and 4.2%, respectively. Based on gully erosion susceptibility derived by RF, more or less equal area of the watershed was devoted to low (27.8%), moderate (28.2%) and high (25.7%) susceptibility classes, while very high classes of susceptibility covered 18% of the total area.

Although only a small portion of the entire area was designated as having a high sensitivity to gully erosion, it can nonetheless have a considerable impact on sediment yield when compared to other classes which is may be attributed to the spatial distribution in the Dodota Alem watershed. Considering all models predicting the spatial distribution of gully erosion susceptibility, the RF models estimated relatively larger areas that fall under very high susceptibility class (18.3%) than the areas that fall under very high susceptibility class (17-30%). However, FR and IoE estimated less area of

proportion under very high gully erosion susceptibility class (nearly 4-8%). Overall, the IoE method appeared to underestimate severe gully erosion features compared to other models.

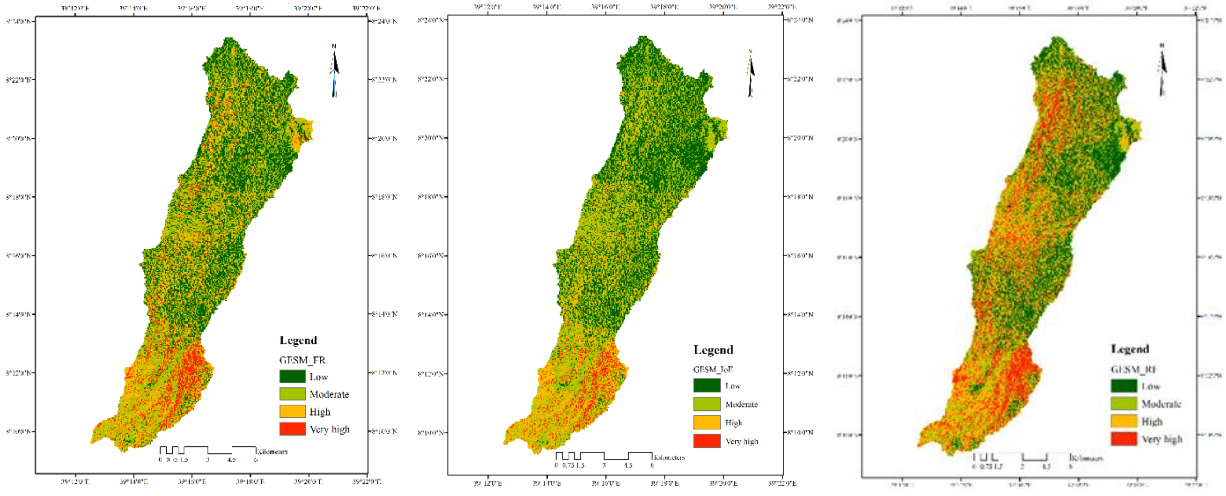

a b c

Figure 4. *Spatial variability of gully erosion susceptibility using three models at Dodota Alem watershed: a) Frequency ratio, b) Index of entropy, c) Random Forest.*

Table 5. *Classification for gully erosion susceptibility for FR, IoE, and RF models.*

Class	FR		IoE		RF	
	Area (ha)	Percent	Area (ha)	Percent	Area (ha)	Percent
Low	4562.0	34.9	4909.2	37.5	3636.8	27.8
Moderate	4237.8	32.4	4882.0	37.3	3686.2	28.2
High	3284.3	25.1	2731.5	20.9	3353.5	25.7
Very high	991.3	7.6	552.6	4.2	2395.4	18.3
Total	13075.3	100	13075.3	100	13072.0	100

3.3. Gully Susceptibility Model Validation

The susceptibility map obtained has been further validated. The area under the curve (AUC) approach was used to evaluate the model accuracy [39]. This curve indicates the accuracy and reliability of a predicting system. [49] classified the AUC values: 0.5–0.6= poor; 0.6–0.7=average; 0.7–0.8=good; 0.8–0.9=very good; and 0.9–1= excellent. For this study, the FR, IoE, and RF models gave AUC values of 0.91, 0.88, and 0.93, respectively (Figure 5). The outcome indicates that FR and RF models have excellent prediction accuracy.

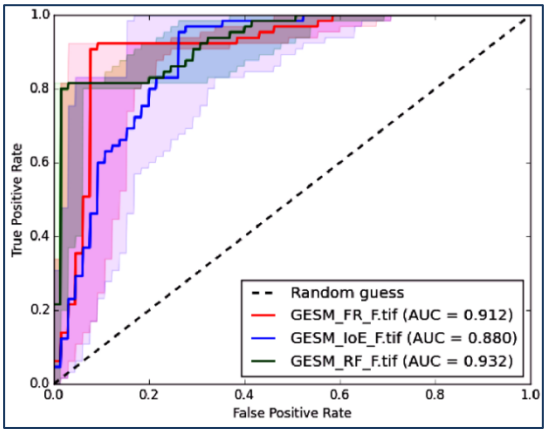

Figure 5. *The area under the curve (AUC) of FR, IoE, and RF models.*

4. Conclusions

The formation of gullies in the study area is not caused by a single factor; rather, all twelve of the geo-environmental factors we looked at were found to be significant for the gully development in the Dodota Alem watershed. VIF and TOL indicate that there is no multi-collinearity among them. The gully erosion susceptibility maps were successfully produced for the study area based on the results of validation using AUC models, which demonstrated their excellent prediction efficiency for all models. However, machine learning (RF) demonstrated the highest accuracy, followed by FR and IoE. Among the factors, distance from roads had the strongest effect on gully erosion susceptibility based on machine learning algorithms of MDG, whereas SPI was the most important factor according to FR and IoE models. The spatial distribution of gully erosion susceptibility classes, when considering all the models, indicates that the majority of the watershed is moderately to highly susceptible to gully erosion.

Therefore, the results of this study can help decision makers and planners to take suitable soil and water conservation measures to reduce the severe problems of land degradation based on the gully erosion susceptibility map. At the same time cost-effective, fast, and well-informed decisions to diminish and evade the damage and losses caused by gully erosion should be planned at the area. Moreover, this approach could be used as a guideline for future research to examine the susceptibility of gully erosion.

Ethical Approval

We confirm that we have given due consideration to the protection of intellectual property associated with this work and that there are no impediments to publication, including the timing of publication, with respect to intellectual property. In so doing we confirm that We have read, understand, and agreed to the submission guidelines, policies, and submission declaration of the journal.

Author Contributions

Gizaw Tesfaye: Conceptualization, Formal Analysis, Supervision, Writing – original draft, Writing – review & editing

Daniel Bekele: Data curation, Formal Analysis, Methodology, Writing – review & editing

Melat Eshetu: Visualization, Writing – review & editing

Mohammed Rabo: Visualization, Writing – review & editing

Abebe Bezu: Visualization, Writing – review & editing

Abera Asefa: Visualization, Writing – review & editing

Funding

The authors declare that no funds, grants, or other support were received during the preparation of this manuscript.

Data Availability Statement

We wish to confirm that all the data and materials related to this study will be available if the needs are raised.

Conflicts of Interest

The authors declare no conflicts of interest.

References

[1] Amare, S., Langendoen, E., Keesstra, S., van der Ploeg, M., Gelagay, H., Lemma, H., van der Zee, S. E. A. T. M., 2021. Susceptibility to gully erosion: Applying random forest (RF) and frequency ratio (FR) approaches to a small catchment in Ethiopia. Water (Switzerland) 13, 1–22. https://doi.org/10.3390/w13020216

[2] Arabameri, A., Blaschke, T., Pradhan, B., Pourghasemi, H. R., Tiefenbacher, J. P., Bui, D. T., 2020a. Evaluation of recent advanced soft computing techniques for gully erosion susceptibility mapping: A comparative study. Sensors (Switzerland) 20, 335–357. https://doi.org/10.3390/s20020335

[3] Arabameri, A., Cerda, A., 2019. Spatial Pattern Analysis and Prediction of Gully Erosion Using Novel Hybrid Model of Entropy-Weight of Evidence. Water 11, 1–23.

[4] Arabameri, A., Chen, W., Loche, M., Zhao, X., Li, Y., Lombardo, L., Cerda, A., Pradhan, B., Tien, D., 2020b. Comparison of machine learning models for gully erosion susceptibility mapping Alireza. Geosci. Front. 11, 1609–1620. https://doi.org/10.1016/j.gsf.2019.11.009

[5] Arabameri, A., Rezaei, K., Pourghasemi, H. R., Lee, S., Yamani, M., 2018. GIS-based gully erosion susceptibility mapping: a comparison among three data-driven models and AHP knowledge-based technique. Environ. Earth Sci. 77, 0. https://doi.org/10.1007/s12665-018-7808-5

[6] Bajocco, S., De Angelis, A., Perini, L., Ferrara, A., Salvati, L., 2012. The impact of Land Use/Land Cover Changes on land degradation dynamics: A Mediterranean case study. Environ. Manage. 49, 980–989. https://doi.org/10.1007/s00267-012-9831-8

[7] Bekele, D., Alamirew, T., Kebede, A., Zeleke, G., M. Melesse, A., 2019. Modeling Climate Change Impact on the Hydrology of Keleta Watershed in the Awash River Basin, Ethiopia. Environ. Model. Assess. 24, 95–107.

[8] Beven, K. J., Kirkby, M. J., 1979. A physically based, variable contributing area model of basin hydrology. Hydrol. Sci. Bull. 24, 43–69. https://doi.org/10.1080/02626667909491834

[9] Borrelli, P., Märker, M., Panagos, P., Schütt, B., 2014. Modeling soil erosion and river sediment yield for an intermountain drainage basin of the Central Apennines, Italy. Catena 114, 45–58. https://doi.org/10.1016/j.catena.2013.10.007

[10] Breiman, L., 2001. Random forest. Lect. Notes Comput. Sci. (including Subser. Lect. Notes Artif. Intell. Lect. Notes Bioinformatics) 45, 5–32. https://doi.org/10.1007/978-3-030-62008-0_35

[11] Busch, R., Hardt, J., Nir, N., Schütt, B., 2021. Modeling Gully Erosion Susceptibility to Evaluate Human Impact on a Local Modeling Gully Erosion Susceptibility to Evaluate Human Impact on a Local Landscape System in Tigray, Ethiopia. Remote Sens. 13, 2009–2029. https://doi.org/10.3390/rs13102009

[12] Caté, A., Perozzi, L., Gloaguen, E., Blouin, M., 2017. Machine learning as a tool for geologists. Lead. Edge 64–68. https://doi.org/10.1190/tle36030215.1

[13] Chen, W., Li, Y., Xue, W., Shahabi, H., Li, S., Hong, H., Wang, X., Bian, H., Zhang, S., Pradhan, B., Ahmad, B. Bin, 2020. Modeling flood susceptibility using data-driven approaches of naïve Bayes tree, alternating decision tree, and random forest methods. Sci. Total Environ. 701, 134979. https://doi.org/10.1016/j.scitotenv.2019.134979

[14] Conforti, M., Aucelli, P. P. C., Robustelli, G., Scarciglia, F., 2011. Geomorphology and GIS analysis for mapping gully erosion susceptibility in the Turbolo stream catchment (Northern Calabria, Italy). Nat. Hazards 56, 881–898. https://doi.org/10.1007/s11069-010-9598-2

[15] Conoscenti, C., Agnesi, V., Angileri, S., Cappadonia, C., Rotigliano, E., Märker, M., 2013. A GIS-based approach for gully erosion susceptibility modelling: A test in Sicily, Italy. Environ. Earth Sci. 70, 1179–1195. https://doi.org/10.1007/s12665-012-2205-y

[16] Cutler, D. R., Beard, K. H., Cutler, A., Gibson, J., 2007. Random Forests for Classification in Ecology. Ecology 88, 2783–2792. https://doi.org/10.1890/07-0539.1

[17] Devkota, K. C., Regmi, A. D., Pourghasemi, H. R., Yoshida, K., Pradhan, B., Ryu, I. C., Dhital, M. R., Althuwaynee, O. F., 2013. Landslide susceptibility mapping using certainty factor, index of entropy and logistic regression models in GIS and their comparison at Mugling-Narayanghat road section in Nepal Himalaya. Nat. Hazards 65, 135–165. https://doi.org/10.1007/s11069-012-0347-6

[18] EMA, 1976. Ethiopian mapping Agency, Topographic Map Series, Addis Ababa, Ethiopia.

[19] Fang, P., Zhang, X., Wei, P., Wang, Y., Zhang, H., Liu, F., Zhao, J., 2020. The classification performance and mechanism of machine learning algorithms in winter wheat mapping using Sentinel-2 10 m resolution imagery. Appl. Sci. 10, 5075–5096. https://doi.org/10.3390/app10155075

[20] FAO/UNESCO, 1995. The Digital Soil Map of the World, Food and Agriculture Organization of the United Nations. Rome, Italy.

[21] Gayen, A., Pourghasemi, H. R., Saha, S., Keesstra, S., Bai, S., 2019. Gully erosion susceptibility assessment and management of hazard-prone areas in India using different machine learning algorithms. Sci. Total Environ. 668, 124–138. https://doi.org/10.1016/j.scitotenv.2019.02.436

[22] Girmay, G., Nyssen, J., Poesen, J., Bauer, H., Merckx, R., Haile, M., Deckers, J., 2012. Land reclamation using reservoir sediments in Tigray, northern Ethiopia. Soil Use Manag. 28, 113–119. https://doi.org/10.1111/j.1475-2743.2011.00368.x

[23] Gómez-Gutiérrez, Á., Conoscenti, C., Angileri, S. E., Rotigliano, E., Schnabel, S., 2015. Using topographical attributes to evaluate gully erosion proneness (susceptibility) in two mediterranean basins: advantages and limitations. Nat. Hazards 79, 291–314. https://doi.org/10.1007/s11069-015-1703-0

[24] Guyassa, E., Frankl, A., Zenebe, A., Poesen, J., Nyssen, J., 2018. Gully and soil and water conservation structure densities in semi-arid northern Ethiopia over the last 80 years. Earth Surf. Process. Landforms 43, 1848–1859.

[25] Haregeweyn, N., Poesen, J., Nyssen, J., De Wit, J., Haile, M., Govers, G., Deckers, S., 2006. Reservoirs in Tigray (Northern Ethiopia): characteristics and sediment deposition problems. L. Degrad. Dev. 17, 211–230. https://doi.org/10.1002/ldr.698

[26] Hosseinalizadeh, M., Kariminejad, N., Chen, W., Pourghasemi, H. R., Alinejad, M., Mohammadian Behbahani, A., Tiefenbacher, J. P., 2019. Gully headcut susceptibility modeling using functional trees, naïve Bayes tree, and random forest models. Geoderma 342, 1–11. https://doi.org/10.1016/j.geoderma.2019.01.050

[27] Hurni, H., 1988. Degradation and conservation of the resources in the Ethiopian highlands. Mt. Res. Dev. 8, 123–130.

[28] Ionita, I., Niacsu, L., Petrovici, G., Blebea-Apostu, A. M., 2015. Gully development in eastern Romania: a case study from Falciu Hills. Nat. Hazards 79, 113–138. https://doi.org/10.1007/s11069-015-1732-8

[29] Jaafari, A., Najafi, A., Pourghasemi, H. R., Rezaeian, J., Sattarian, A., 2014. GIS-based frequency ratio and index of entropy models for landslide susceptibility assessment in the Caspian forest, northern Iran. Int. J. Environ. Sci. Technol. 11, 909–926. https://doi.org/10.1007/s13762-013-0464-0

[30] Jenks, G. F., Caspall, F. C., 1971. Error on choroplethic maps: definition, measurement, reduction. Ann. Assoc. Am. Geogr. 61, 217–244. https://doi.org/10.1111/j.1467-8306.1971.tb00779.x

[31] Joseph, S., Anitha, K., Srivastava, V. K., Reddy, C. S., Thomas, A. P., Murthy, M. S. R., 2012. Rainfall and Elevation Influence the Local-Scale Distribution of Tree Community in the Southern Region of Western Ghats Biodiversity Hotspot (India). Int. J. For. Res. 2012, 1–10. https://doi.org/10.1155/2012/576502

[32] Lai, J. S., Tsai, F., 2019. Improving GIS-based landslide susceptibility assessments with multi-temporal remote sensing and machine learning. Sensors (Switzerland) 19, 1–26. https://doi.org/10.3390/s19173717

[33] Lawrence, R. L., Wood, S. D., Sheley, R. L., 2006. Mapping invasive plants using hyperspectral imagery and Breiman Cutler classifications (RandomForest). Remote Sens. Environ. 100, 356–362. https://doi.org/10.1016/j.rse.2005.10.014

[34] Liaw, A., Wiener, M., 2002. Classification and Regression by randomForest. R News 2, 18–22.

[35] Luffman, I. E., Nandi, A., Spiegel, T., 2015. Gully morphology, hillslope erosion, and precipitation characteristics in the Appalachian Valley and Ridge province, southeastern USA. Catena 133, 221–232. https://doi.org/10.1016/j.catena.2015.05.015

[36] Mekonnen, M., Keesstra, S. D., Baartman, J. E. M., Stroosnijder, L., Maroulis, J., 2017. Reducing Sediment Connectivity Through man-Made and Natural Sediment Sinks in the Minizr Catchment, Northwest Ethiopia. L. Degrad. Dev. 28, 708–717. https://doi.org/10.1002/ldr.2629

[37] Moeini, A., Zarandi, N. K., Pazira, E., Badiollahi, Y., 2015. The relationship between drainage density and soil erosion rate: a study of five watersheds in Ardebil Province, Iran. River Basin Manag. VIII 197, 129–138. https://doi.org/10.2495/rm150121

[38] Mohammady, M., Pourghasemi, H. R., Amiri, M., 2019. Land subsidence susceptibility assessment using random forest machine learning algorithm. Environ. Earth Sci. 78, 1–12. https://doi.org/10.1007/s12665-019-8518-3

[39] Mohammady, M., Pourghasemi, H. R., Pradhan, B., 2012. Landslide susceptibility mapping at Golestan Province, Iran: A comparison between frequency ratio, Dempster–Shafer, and weights-of-evidence models. J. Asian Earth Sci. 61, 221–236. https://doi.org/10.1016/j.jseaes.2012.10.005

[40] Moore, I. D., Grayson, R. B., Ladson, A. R., 1991. Digital terrain modelling: A review of hydrological, geomorphological, and biological applications. Hydrol. Process. 5, 3–30.

[41] Morgan, R. P. C., 2005. Soil Erosion and Conservation, 3rd ed. Blackwell Publishing Ltd, Oxford, UK.

[42] Nyssen, J., Moeyersons, J., Deckers, J., Haile, M., Poesen, J., 2000. Vertic movements and the development of stone covers and gullies, Tigray Highlands, Ethiopia. Zeitschrift für Geomorphol. 44, 145–164. https://doi.org/10.1127/zfg/44/2000/145

[43] Nyssen, J., Poesen, J., Moeyersons, J., Haile, M., Deckers, J., 2008. Dynamics of soil erosion rates and controlling factors in the Northern Ethiopian Highlands – towards a sediment budget. Earth Surf. Process. Landforms 33, 695–711. https://doi.org/doi.org/10.1002/esp.1569

[44] O'brien, R. M., 2007. A Caution Regarding Rules of Thumb for Variance Inflation Factors. Qual. Quant. 41, 673–690. https://doi.org/10.1007/s11135-006-9018-6

[45] Pathak, P., Wani, S. P., Sudi, R. S., 2006. Gully Control in SAT Watersheds.

[46] Peckham, S., 2011. Profile, plan and streamline curvature: a simple derivation and applications, in: Geomorphometry 2011. pp. 27–30.

[47] Pourghasemi, H. R., Yousefi, S., Kornejady, A., Cerdà, A., 2017. Performance assessment of individual and ensemble data-mining techniques for gully erosion modeling. Sci. Total Environ. 609, 764–775. https://doi.org/10.1016/j.scitotenv.2017.07.198

[48] Rahmati, O., Kalantari, Z., Ferreira, C. S., Chen, W., Soleimanpour, S. M., Kapović-Solomun, M., Seifollahi-Aghmiuni, S., Ghajarnia, N., Kazemi Kazemabady, N., 2022. Contribution of physical and anthropogenic factors to gully erosion initiation. Catena 210, 105925–105936. https://doi.org/10.1016/j.catena.2021.105925

[49] Rahmati, O., Tahmasebipour, N., Haghizadeh, A., Pourghasemi, H. R., Feizizadeh, B., 2017. Evaluation of different machine learning models for predicting and mapping the susceptibility of gully erosion. Geomorphology 298, 118–137. https://doi.org/10.1016/j.geomorph.2017.09.006

[50] Saha, S., 2017. Groundwater potential mapping using analytical hierarchical process: a study on Md. Bazar Block of Birbhum District, West Bengal. Spat. Inf. Res. 25, 615–626. https://doi.org/10.1007/s41324-017-0127-1

[51] Tamene, L., Abera, W., Demissie, B., Desta, G., Woldearegay, K., Mekonnen, K., 2022. Soil erosion assessment in Ethiopia: A review. J. Soil Water Conserv. 77, 144–157. https://doi.org/10.2489/jswc.2022.00002

[52] Tamene, L., Vlek, P. L. G., 2007. Assessing the potential of changing land use for reducing soil erosion and sediment yield of catchments: A case study in the highlands of northern Ethiopia. Soil Use Manag. 23, 82–91. https://doi.org/10.1111/j.1475-2743.2006.00066.x

[53] Trigila, A., Iadanza, C., Esposito, C., Scarascia-Mugnozza, G., 2015. Comparison of Logistic Regression and Random Forests techniques for shallow landslide susceptibility assessment in Giampilieri (NE Sicily, Italy). Geomorphology 249, 119–136. https://doi.org/10.1016/j.geomorph.2015.06.001

[54] Valentin, C., Poesen, J., Li, Y., 2005. Gully erosion: Impacts, factors and control. Catena 63, 132–153. https://doi.org/10.1016/j.catena.2005.06.001

[55] van den Ham, J.-P., 2008. Dodota Spate Irrigation System Ethiopia A case study of. Wageningen university.

[56] Wang, D., Fan, H., Fan, X., 2017. Distributions of recent gullies on hillslopes with different slopes and aspects in the Black Soil Region of Northeast China. Environ. Monit. Assess. 189, 508–523. https://doi.org/10.1007/s10661-017-6221-y

[57] Wang, L., Wei, S., Horton, R., Shao, M., 2011. Effects of vegetation and slope aspect on water budget in the hill and gully region of the Loess Plateau of China. Catena 87, 90–100. https://doi.org/10.1016/j.catena.2011.05.010

[58] Wang, Q., Li, W., Wu, Y., Pei, Y., Xie, P., 2016. Application of statistical index and index of entropy methods to landslide susceptibility assessment in Gongliu (Xinjiang, China). Environ. Earth Sci. 75, 599–612. https://doi.org/10.1007/s12665-016-5400-4

[59] Yibeltal, M., Tsunekawa, A., Haregeweyn, N., Adgo, E., Meshesha, D. T., Aklog, D., Masunaga, T., Tsubo, M., Billi, P., Vanmaercke, M., Ebabu, K., Dessie, M., Sultan, D., Liyew, M., 2019. Analysis of long-term gully dynamics in different agro-ecology settings. Catena 179, 160–174. https://doi.org/10.1016/j.catena.2019.04.013

[60] Zabihi, M., Mirchooli, F., Motevalli, A., Khaledi Darvishan, A., Pourghasemi, H. R., Zakeri, M. A., Sadighi, F., 2018. Spatial modelling of gully erosion in Mazandaran Province, northern Iran. Catena 161, 1–13. https://doi.org/10.1016/j.catena.2017.10.010

[61] Zeleke, G. and, Hurni, H., 2001. Implications of land use and land cover dynamics for mountain resource degradation in the Northwestern Ethiopian highlands. Mt. Res. Dev. 21, 184–191.

[62] Zheng, F.-L., 2006. Effect of Vegetation Changes on Soil Erosion on the Loess Plateau1 1Project supported by the Chinese Academy of Sciences (No. KZCX3-SW-422) and the National Natural Science Foundation of China (Nos. 9032001 and 40335050). Pedosphere 16, 420–427. https://doi.org/https://doi.org/10.1016/S1002-0160(06)60071-4